

May 13, 2022



USGS 3DEP Umatilla, Union, & Morrow, Oregon NIR Lidar Technical Data Report

Task Order: 140G00221F0079

Project ID: 218279

Contract: G16PC00016

Work Unit ID: 218276

Prepared For:



United States Geological Survey
1400 Independence Road
Rolla, MO 65401

Prepared By:



NV5 Geospatial Corvallis
1100 NE Circle Blvd, Ste. 126
Corvallis, OR 97330
PH: 541-752-1204

TABLE OF CONTENTS

INTRODUCTION	1
Deliverable Products	2
ACQUISITION	4
Planning.....	4
Airborne Lidar Survey.....	7
Ground Survey.....	9
Base Stations.....	9
Ground Survey Points (GSPs).....	11
Land Cover Class	12
PROCESSING	16
Lidar Data	16
Feature Extraction	19
Hydroflattening and Water’s Edge Breaklines.....	19
RESULTS & DISCUSSION.....	20
Lidar Density.....	20
Lidar Accuracy Assessments.....	24
Lidar Non-Vegetated Vertical Accuracy.....	24
Lidar Vegetated Vertical Accuracies	27
Lidar Relative Vertical Accuracy	29
Lidar Horizontal Accuracy	30
CERTIFICATIONS	31
GLOSSARY	32
APPENDIX A - ACCURACY CONTROLS	33

Cover Photo: A view looking north towards Hawkins Point over the south fork of the Imnaha River in the Eagle Cap Wilderness Area inside of the Wallowa-Whitman National Forest. This image was created using lidar ground returns to produce a 3-dimensional bare earth surface model, was and colored by elevation and shaded by lidar ground return intensity values.

INTRODUCTION

A scenic photo taken by NV5 Acquisition Staff showing Anthony Lake within the Umatilla 3DEP site (taken June 28, 2021)



In April 2021 NV5 Geospatial (NV5) was contracted by the United States Geologic Survey (USGS) to collect Quality Level 1 (QL1) high resolution NIR Light Detection and Ranging (lidar) data. The acquisition took place during the Spring and Summer of 2021 for the Umatilla, Union, & Morrow site in northeastern Oregon near the Washington border. The defined project area (DPA) includes the Blue and Wallowa Mountains and spans across three counties (Umatilla, Union, and Morrow). Morrow County sits on the western side of the boundary, Umatilla County to the northeastern edge, and Union County in the southwestern part of the boundary. The area is diverse, containing grasslands, forested areas, rolling hills, shrubs, and urban areas. This project supports the USGS 3DEP mission to obtain elevation data to better manage and protect lives, property, and the environment as well as improve planning for future projects.

This report accompanies the delivered lidar data, and documents contract specifications, data acquisition procedures, processing methods, and analysis of the final dataset including lidar accuracy and density. Acquisition dates and buffered acreage are shown in Table 1, a complete list of contracted deliverables provided to USGS is shown in Table 2, and the buffered area of interest (AOI) is shown in Figure 1.

Table 1: Acquisition dates, acreage, and data types collected on the Umatilla, Union, & Morrow site

Project Site	Contracted Acres	Acquisition Dates	Data Type
USGS 3DEP Umatilla, Union, & Morrow, Oregon	3,053,120	04/15/2020 – 09/03/2021*	NIR-Lidar

*Please see Table 3 for more detailed flight date information.

Deliverable Products

Table 2: Products delivered to USGS for the Umatilla, Union, & Morrow site

Umatilla, Union, & Morrow Projection: UTM Zone 11 North Horizontal Datum: NAD83 (2011) Vertical Datum: NAVD88 (GEOID18) Units: Meters	
Data Type	NIR - Lidar
Points	LAS v 1.4 <ul style="list-style-type: none"> • All Classified Returns
Rasters	0.5 Meter Cloud Optimized GeoTiffs <ul style="list-style-type: none"> • Hydroflattened Bare Earth Model (DEM) • Maximum Surface Height Model (DSM) • Intensity Images • Swath Separation Images
Vectors	Shapefiles (*.shp) <ul style="list-style-type: none"> • Defined Project Area • Master Tile Index ESRI Geodatabase (*.gdb) <ul style="list-style-type: none"> • 3D Hydroflattened-Breaklines • 3D Bridge Breaklines • Flightline Swath Coverage Extents • Flightline Index Geopackage (*.gpkg) <ul style="list-style-type: none"> • Ground Survey Shapes

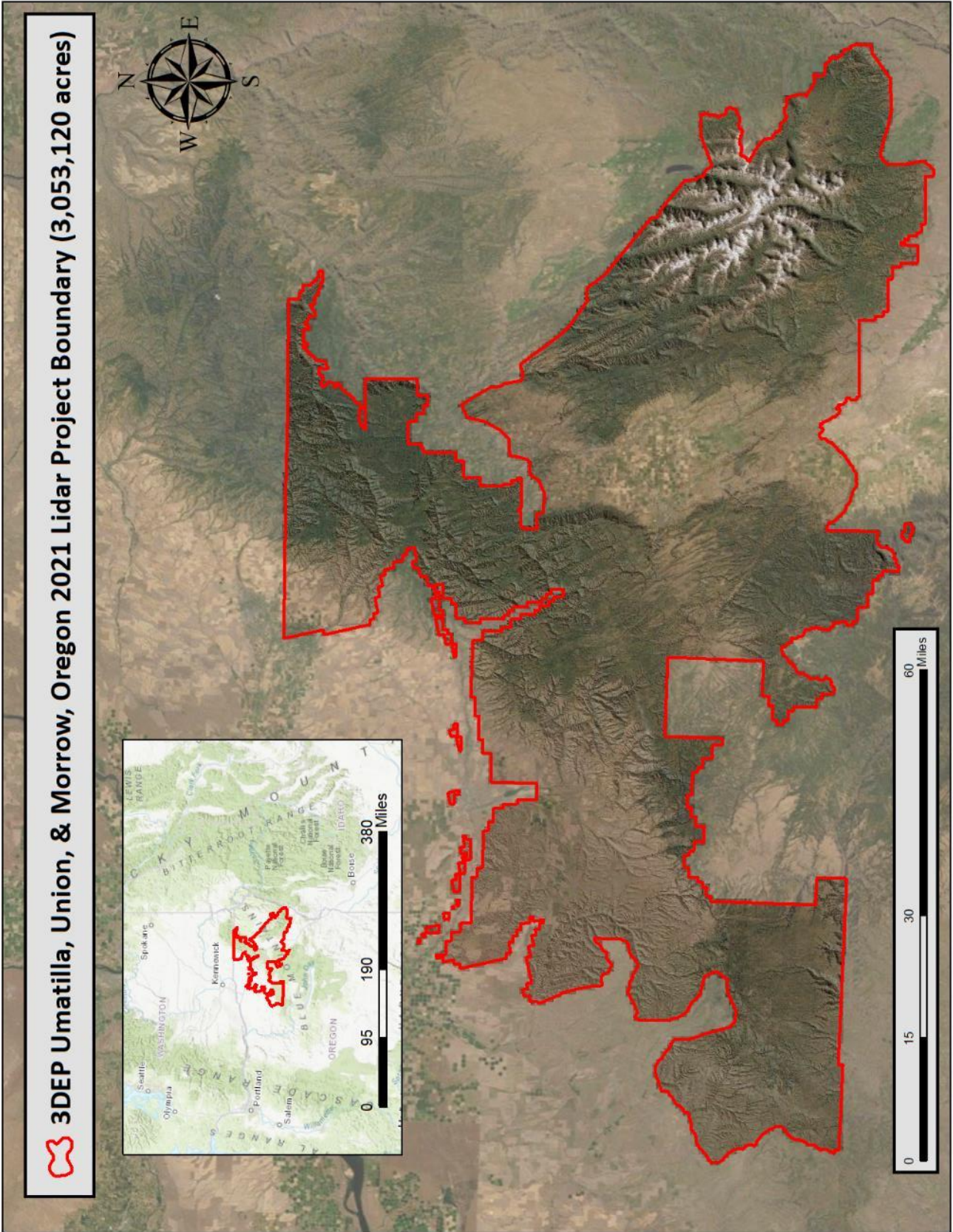


Figure 1: Location map of the Umatilla, Union, & Morrow site in Oregon

An image of NV5's ground acquisition equipment set up in the Umatilla, Union, and Morrow AOI (taken June 11, 2021).



Planning

In preparation for data collection, NV5 Geospatial reviewed the project area and developed a specialized flight plan to ensure complete coverage of the Umatilla, Union, & Morrow lidar study area at the target point density of ≥ 8.0 points/m². Acquisition parameters including orientation relative to terrain, flight altitude, pulse rate, scan angle, and ground speed were adapted to optimize flight paths and flight times while meeting all contract specifications.

Factors such as satellite constellation availability and weather windows must be considered during the planning stage. Any weather hazards or conditions affecting the flights were continuously monitored due to their potential impact on the daily success of airborne and ground operations. Flights were planned to occur during beneficial weather window when heavy clouds dissipated to ensure there was no adverse effect on crew safety or the collection of quality Lidar data. Due to these conditions, the flight dates are not continuous. In addition, proper sensors were used to handle light snow conditions when complete snow off conditions were not achievable. In addition, logistical considerations including private property access and potential air space restrictions were reviewed. Table 3 shows the flight line dates, start time, and end time, while Figure 2 illustrates where and when flights occurred for the project.

Table 3: Flight Date Table

Date	Flight Line Number	Start Time (Adjusted GPS)	End Time (Adjusted GPS)
4/15/2021	100 - 110	302531546	302537891
4/16/2021	200 - 221	302603626	302619329
4/18/2021	300 - 315	302776816	302786884
4/19/2021	400 - 411, 414 - 420, 422	302870547	302882315
4/20/2021	500 - 513, 515 - 523	302944188	302958166
5/6/2021	601 - 628	304333761	304349980
5/8/2021	700 - 712	304528792	304536017
6/8/2021	800 - 818, 820 - 836	307201597	307216673
7/7/2021	1000 - 1023	309686818	309704084
7/12/2021	1100 - 1116	310120527	310132857
7/13/2021	1200 - 1203, 1205 - 1234, 1236	310199661	310219094
7/16/2021	1300 - 1309	310478799	310483680
7/17/2021	1400 - 1417, 1419 - 1429	310550803	310566149
7/18/2021	1500 - 1505	310637650	310639791
7/30/2021	1600 - 1619, 1621 - 1635	311672654	311692242
7/31/2021	1700 - 1721, 1723 - 1724, 1726 - 1735, 1737 - 1739	311758031	311778500
8/7/2021	1800 - 1804, 1806 - 1837	312364356	312381310
8/8/2021	1900 - 1919	312464711	312479783
8/9/2021	2000 - 2018, 2020 - 2022	312537820	312555829
8/10/2021	2100 - 2123	312623873	312639761
8/11/2021	2200 - 2215, 2217 - 2221	312710605	312726775
8/12/2021	2300 - 2327	312798205	312813548
8/15/2021	2400 - 2418, 2420 - 2423, 2425 - 2431	313059575	313075793
8/16/2021	2800 - 2807, 2809 - 2818, 2820 - 2829	313144287	313160257
8/17/2021	2600 - 2607, 2610 - 2611	313248215	313254332
8/19/2021	2500 - 2512	313398860	313407575
8/20/2021	2701 - 2712, 2714 - 2717	313488013	313499447
8/22/2021	2900 - 2907, 3000 - 3007, 3009 - 3011	313659837	313669367
8/23/2021	3100 - 3126	313745495	313759429
8/26/2021	3200 - 3214	314015199	314023832

Table 3: Flight Date Table

Date	Flight Line Number	Start Time (Adjusted GPS)	End Time (Adjusted GPS)
8/28/2021	3301 - 3326	314173723	314192015
8/29/2021	3400 - 3426, 3428	314260856	314278819
8/30/2021	3500 - 3527	314343374	314357514
8/31/2021	3600 - 3626	314430006	314447303
9/1/2021	3900 - 3925	314521133	314537805
9/2/2021	3800 - 3829	314608834	314623232
9/3/2021	3700 - 3715	314705479	314711380

Airborne Lidar Survey

The lidar survey was accomplished using Riegl VQ-1560-ii and ii-S laser systems mounted in a Cessna Caravan. Table 4 summarizes the settings used to yield USGS QL-1 standards of an average pulse density of ≥ 8 pulses/m² over the Umatilla, Union, & Morrow project area. The Riegl VQ-1560-ii and ii-S laser systems can record unlimited range measurements (returns) per pulse, however a maximum of 15 returns can be stored due to LAS v1.4 file limitations. It is not uncommon for some types of surfaces (e.g., dense vegetation or water) to return fewer pulses to the lidar sensor than the laser originally emitted. The discrepancy between first return and overall delivered density will vary depending on terrain, land cover, and the prevalence of water bodies. All discernible laser returns were processed for the output dataset.

Table 4: Lidar specifications and survey settings

2021 Lidar Survey Settings & Specifications		
Acquisition Dates	4/15-4/16, 4/18-4/20, 5/6, 5/8, 6/8, 7/30, 7/31, 8/7-8/12, 8/15-8/17, 8/19-8/20, 8/22-8/23, 8/26, 8/28-9/3	7/7/2021 – 7/18/2021
Aircraft Used	Cessna Caravan	Cessna Caravan
Sensor	Riegl	Riegl
Laser	VQ-1560-ii	VQ-1560-iis
Maximum Returns	15	15
Resolution/Density	Average 8 pulses/m ²	Average 8 pulses/m ²
Nominal Pulse Spacing	0.35 m	0.35 m
Survey Altitude (AGL)	2,085 m	2,365 m
Survey speed	145 knots	145 knots
Field of View	58.5 °	58.5 °
Mirror Scan Rate	Uniform Point Spacing	Uniform Point Spacing
Target Pulse Rate	634 kHz	721 kHz
Pulse Length	3 ns	3 ns
Laser Pulse Footprint Diameter	37.5 cm	40.2 cm
Central Wavelength	1064 nm	1064 nm
Pulse Mode	Multiple Times Around (MTA)	Multiple Times Around (MTA)
Beam Divergence	0.18 mrad	0.17 mrad
Swath Width	2,335 m	2,649 m
Swath Overlap	55%	55%
Intensity	16-bit	16-bit
Accuracy	RMSE _z (Non-Vegetated) ≤ 10 cm	RMSE _z (Non-Vegetated) ≤ 10 cm
	NVA (95% Confidence Level) ≤ 19.6 cm	NVA (95% Confidence Level) ≤ 19.6 cm
	VVA (95 th Percentile) ≤ 30 cm	VVA (95 th Percentile) ≤ 30 cm

All areas were surveyed with an opposing flight line side-lap of $\geq 50\%$ ($\geq 100\%$ overlap) in order to reduce laser shadowing and increase surface laser painting. To accurately solve for laser point position (geographic coordinates x, y and z), the positional coordinates of the airborne sensor and the attitude of the aircraft were recorded continuously throughout the lidar data collection mission. Position of the aircraft was measured twice per second (2 Hz) by an onboard differential GPS unit, and aircraft attitude was measured 200 times per second (200 Hz) as pitch, roll and yaw (heading) from an onboard inertial measurement unit (IMU). To allow for post-processing correction and calibration, aircraft and sensor position and attitude data are indexed by GPS time.

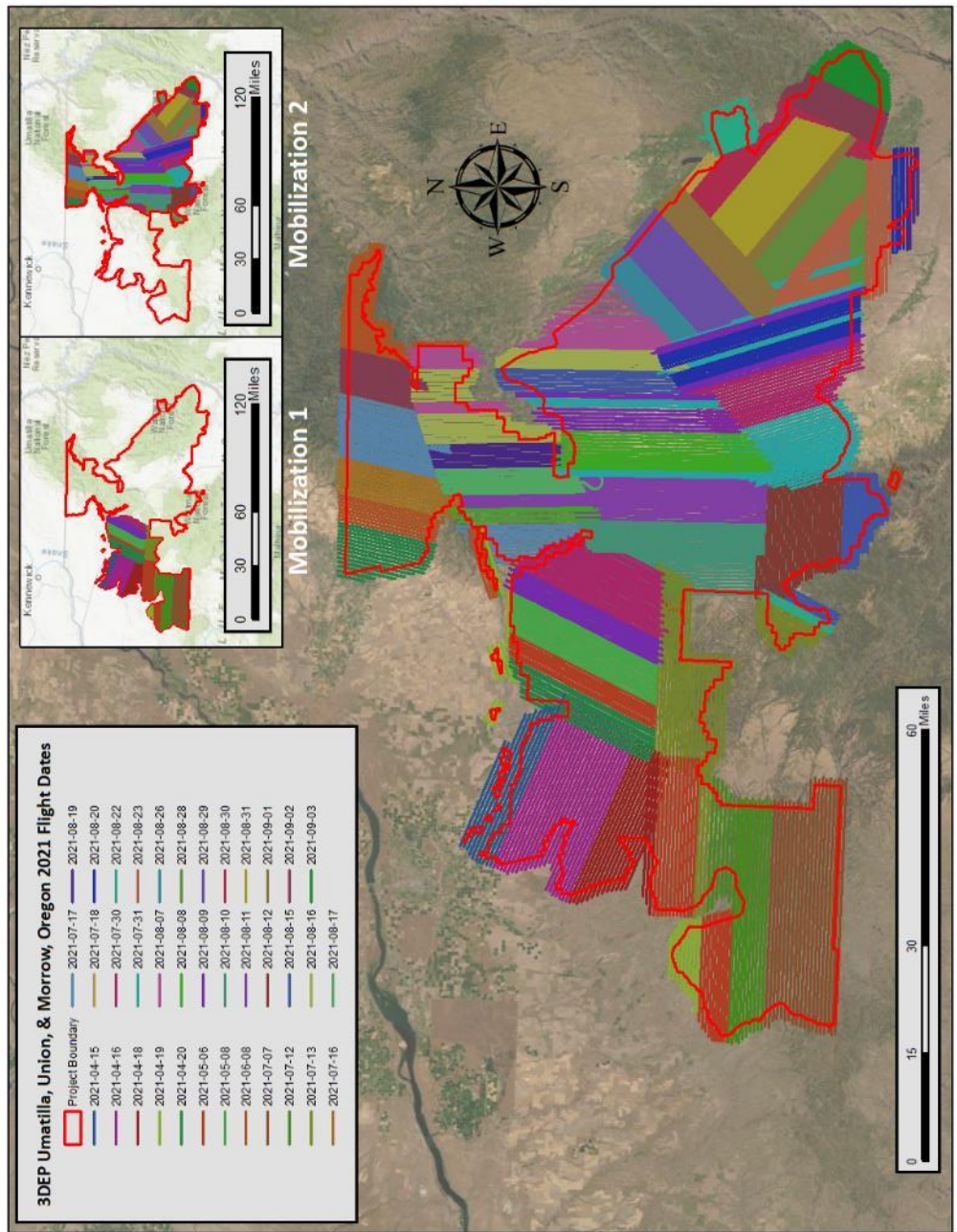


Figure 2: Flightline Map

Ground Survey

Ground control surveys, including monumentation, and ground survey points (GSPs) were conducted to support the airborne acquisition. Ground control data were used to geospatially correct the aircraft positional coordinate data and to perform quality assurance checks on final lidar data.



NV5 Geospatial Monument

Base Stations

Base stations were utilized for collection of ground survey points using real time kinematic (RTK), fast static (FS), and total station (TS) survey techniques.

Monument locations were selected with consideration for satellite visibility, field crew safety, and optimal location for GSP coverage. NV5 Geospatial utilized ten permanent real-time network (RTN) base stations from the Oregon Real-time GNSS Network (ORGN) and two from the Leica SmartNet network. NV5 Geospatial also established ten new monuments using 6" mag hub nails with orange survey washers, and utilized two existing monuments – one existing NV5 monument set using 5/8" x 30" rebar topped with stamped 2 ½ " aluminum caps, and one NGS monument (Table 5, Figure 3). NV5 Geospatial's professional land surveyor, Evon Silvia (ORPLS#81104) oversaw the ground survey and certified the establishment of all monuments.

NV5 Geospatial utilized static Global Navigation Satellite System (GNSS) data collected at 1 Hz recording frequency for each base station. During post-processing, the static GNSS data were triangulated with nearby Continuously Operating Reference Stations (CORS) using the Online Positioning User Service (OPUS¹) for precise positioning. Multiple independent sessions over the same monument were processed to confirm antenna height measurements and to refine position accuracy.

¹ OPUS is a free service provided by the National Geodetic Survey to process corrected monument positions.

<http://www.ngs.noaa.gov/OPUS>.

Table 5: Base station positions for the Umatilla, Union, & Morrow acquisition. Coordinates are on the NAD83 (2011) datum, epoch 2011.00.

Monument ID	Owner	Latitude	Longitude	Ellipsoid (meters)
GRANDERONDE_01	NV5 AL Cap	45° 07' 28.48297"	-118° 24' 09.73070"	1716.444
GRANDERONDE_03	NV5 AL Cap	45° 20' 51.43296"	-118° 13' 18.25130"	891.243
GRANDERONDE_04	NV5 AL Cap	45° 15' 23.67625"	-118° 24' 33.09118"	1019.138
GRANDERONDE_07	NV5 AL Cap	45° 08' 37.58917"	-117° 42' 26.50403"	1103.04
UMA_02	NV5 AL Cap	45° 46' 36.71318"	-118° 02' 41.44893"	1579.463
UMATILLA_11	NV5 AL Cap	45° 26' 26.20193"	-118° 20' 28.29262"	1250.504
USGS_UUM_01	NV5 AL Cap	45° 23' 26.73388"	-119° 10' 42.96493"	1015.157
USGS_UUM_02	NV5 Nail	45° 15' 27.52448"	-119° 29' 18.10733"	1016.868
USGS_UUM_03	NV5 Nail	45° 03' 17.49418"	-119° 33' 40.99636"	1280.992
USGS_UUM_04	NV5 Nail	45° 10' 11.82303"	-119° 08' 16.79606"	1462.053
USGS_UUM_05	NV5 Nail	45° 56' 37.71099"	-118° 00' 56.18926"	1468.086
USGS_UUM_06	NV5 Nail	44° 58' 23.24230"	-117° 23' 23.11674"	1546.487
USGS_UUM_07	NV5 Nail	45° 02' 12.31338"	-117° 03' 53.42406"	1997.296
USGS_UUM_08	NV5 Nail	44° 58' 31.99641"	-118° 08' 19.53460"	1672.435
USGS_UUM_09	NV5 Nail	45° 36' 04.28834"	-118° 09' 26.00673"	1542.380
USGS_UUM_10	NV5 Nail	45° 20' 21.46802"	-118° 45' 27.15203"	1574.831
ELG2	ORGN	45° 33' 53.49145"	-117° 55' 42.27526"	816.489
ENTR	ORGN	45° 25' 52.50655"	-117° 17' 17.03741"	1127.055
HALF	ORGN	44° 52' 20.58922"	-117° 05' 59.32893"	783.937
P022	ORGN	45° 13' 54.41272"	-118° 00' 49.52589"	888.603
P394	ORGN	44° 50' 05.55486"	-117° 47' 58.64029"	1011.194
P450	ORGN	45° 57' 11.98969"	-119° 32' 39.04141"	164.111
PDTN	ORGN	45° 39' 57.39193"	-118° 45' 24.88380"	394.909
SPRA	ORGN	44° 49' 36.07476"	-119° 46' 34.64026"	567.247
UKIA	ORGN	45° 07' 58.05613"	-118° 56' 11.63734"	1009.481
WALA	ORGN	46° 05' 29.42010"	-118° 15' 29.25508"	369.235
ORHP	SmartNet	45° 21' 38.66331"	-119° 33' 54.55586"	606.163
ORPE	SmartNet	45° 40' 15.33056"	-118° 51' 00.63592"	312.577
WAWL	SmartNet	46° 04' 54.53745"	-118° 16' 55.93283"	338.905

Monuments were established according to the national standard for geodetic control networks, as specified in the Federal Geographic Data Committee (FGDC) Geospatial Positioning Accuracy Standards for geodetic networks.² This standard provides guidelines for classification of monument quality at the 95% confidence interval as a basis for comparing the quality of one control network to another. The monument rating for this project is shown in Table 6.

Table 6: Federal Geographic Data Committee monument rating for network accuracy

Direction	Rating
1.96 * St Dev _{NE} :	0.020 m
1.96 * St Dev _Z :	0.050 m

For the Umatilla, Union, & Morrow Lidar project, the monument coordinates contributed no more than 5.6 cm of positional error to the geolocation of the final ground survey points and lidar, with 95% confidence.

Ground Survey Points (GSPs)

Ground survey points were collected using real time kinematic (RTK), fast-static (FS), and total station (TS) survey techniques. For RTK surveys, a roving receiver receives corrections from a nearby base station or Real-Time Network (RTN) via radio or cellular network, enabling rapid collection of points with relative errors less than 1.5 cm horizontal and 2.0 cm vertical. FS surveys compute these corrections during post-processing to achieve comparable accuracy. RTK surveys record data while stationary for at least five seconds, calculating the position using at least three one-second epochs. FS surveys record observations for up to fifteen minutes on each GSP to support longer baselines. All GSP measurements were made during periods with a Position Dilution of Precision (PDOP) of ≤ 3.0 with at least six satellites in view of the stationary and roving receivers. See Table 7 for ground survey equipment specifications. Forested check points are collected using total stations to measure positions under dense canopy. Total station backsight and setup points are established using GNSS survey techniques.

GSPs were collected in areas where good satellite visibility was achieved on paved roads and other hard surfaces such as gravel or packed dirt roads. GSP measurements were not taken on highly reflective surfaces such as center line stripes or lane markings on roads due to the increased noise seen in the laser returns over these surfaces. GSPs were collected within as many flightlines as possible; however, the distribution of GSPs depended on ground access constraints and monument locations and may not be equably distributed throughout the study area (Figure 3).

² Federal Geographic Data Committee, Geospatial Positioning Accuracy Standards (FGDC-STD-007.2-1998). Part 2: Standards for Geodetic Networks, Table 2.1, page 2-3. <http://www.fgdc.gov/standards/projects/FGDC-standards-projects/accuracy/part2/chapter2>

Table 7: NV5 Geospatial ground survey equipment identification

Receiver Model	Antenna	OPUS Antenna ID	Use
Trimble R7	Zephyr GNSS Geodetic Model 2 RoHS	TRM57971.00	Static
Trimble R10 Model 2	Integrated Antenna	TRMR10-2	Rover
Trimble R8 Model 3	Integrated Antenna	TRMR8_GNSS3	Static, Rover
Nikon NPL-322+ 5" P Total Station		n/a	VVA

Land Cover Class

In addition to ground survey points, land cover class check points were collected throughout the study area to evaluate vertical accuracy. Vertical accuracy statistics were calculated for all land cover types to assess confidence in the lidar derived ground models across land cover classes Table 8 and Figure 4, (see Lidar Accuracy Assessments, page 24). Quality assurance photographs were taken at each ground checkpoint during the day at the time of acquisition in each direction (North, South, East, and West). Table 8 shows an example of this for each land class type.

Table 8: Land Cover Types and Descriptions

Land Cover Type	Land Cover Code	Example	Description	Accuracy Assessment Type
Shrub	SH		Low growth shrub	VVA
Tall Grass	TG		Herbaceous grasslands in advanced stages of growth	VVA
Forest	FR		Forested areas	VVA
Bare Earth	BE		Areas of bare earth surface	NVA
Urban	UA		Areas dominated by urban development, including parks	NVA

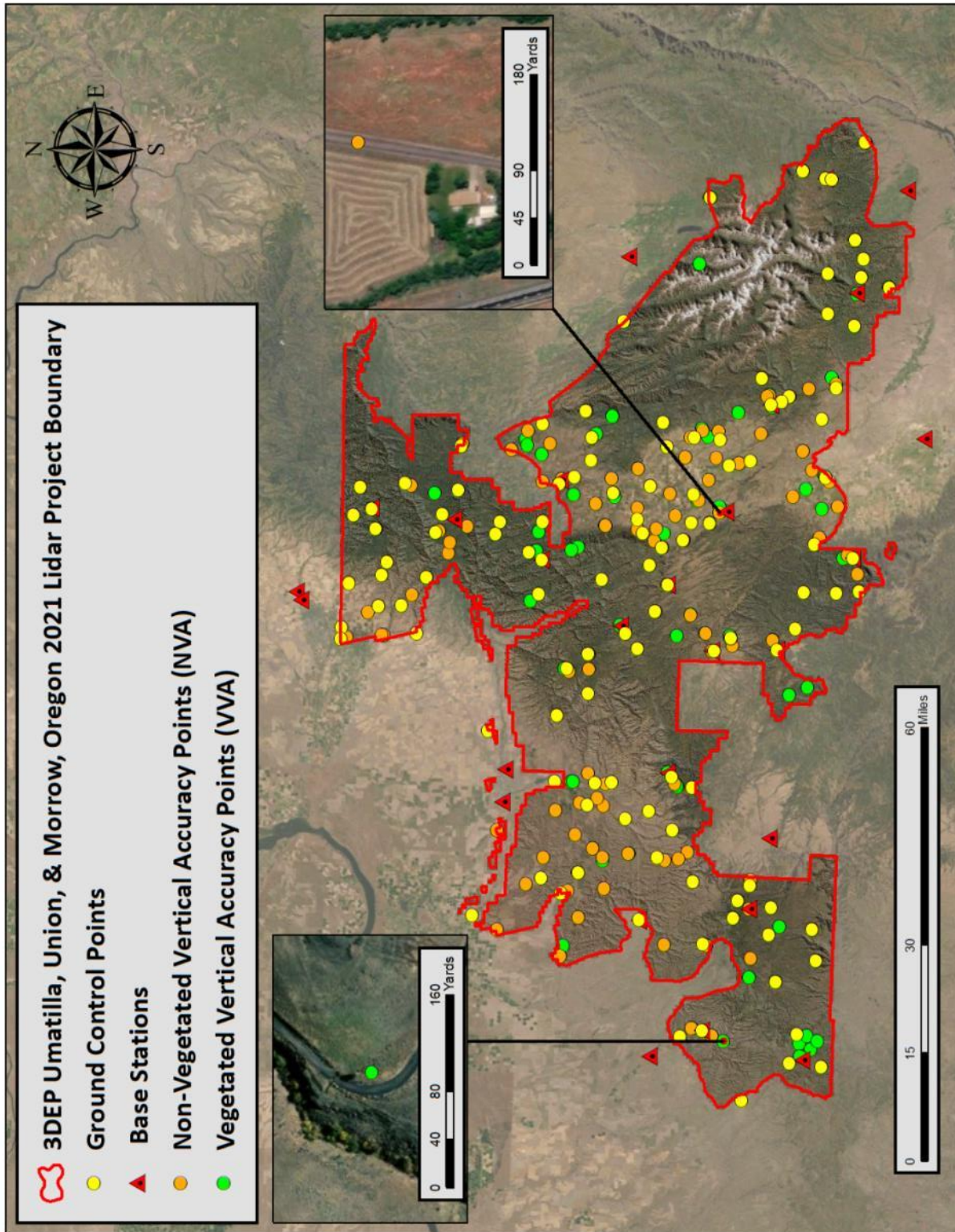


Figure 3: Ground survey location map

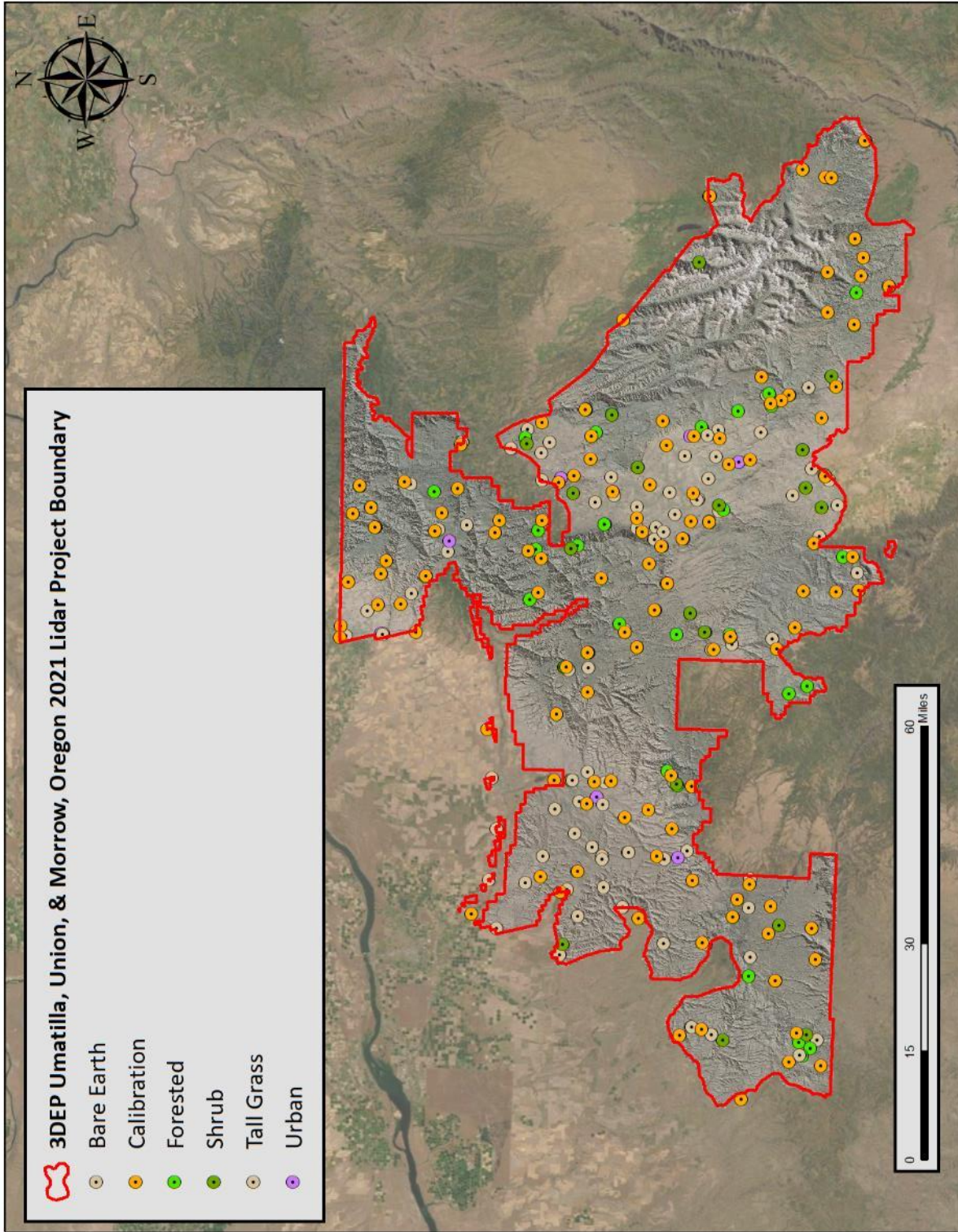
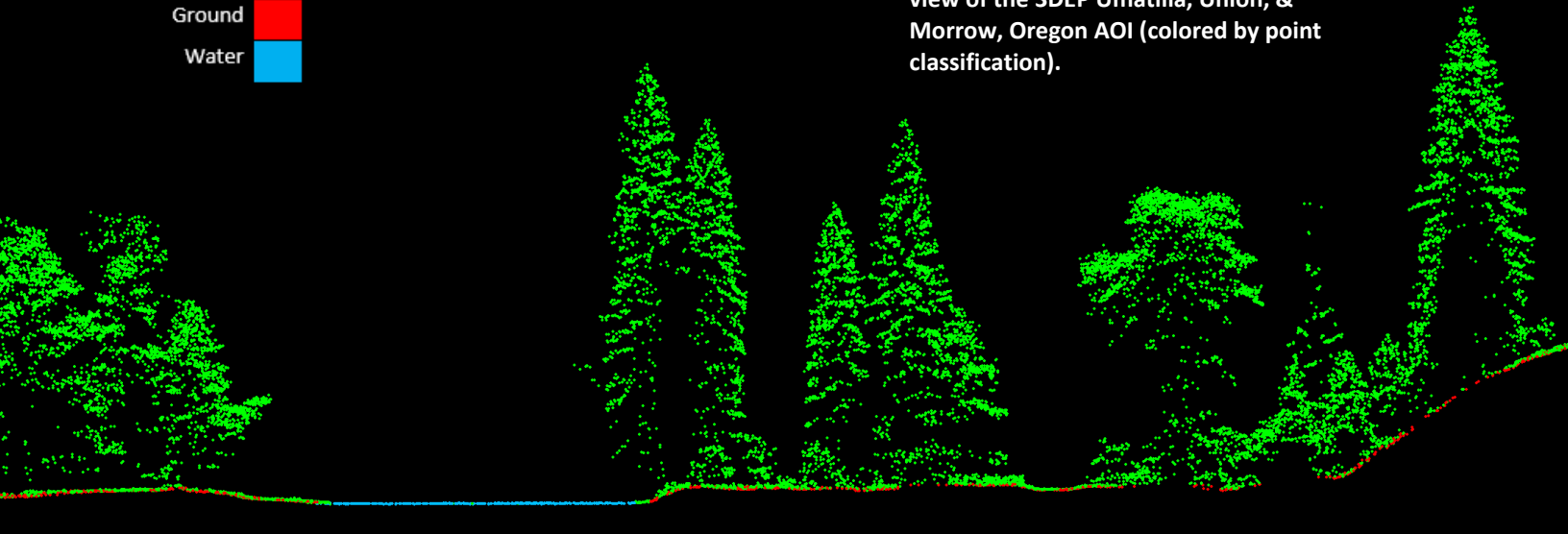


Figure 4: Map showing the land cover type locations in the AOI

PROCESSING

Default 
Ground 
Water 

This 2 meter lidar cross section shows a view of the 3DEP Umatilla, Union, & Morrow, Oregon AOI (colored by point classification).



Lidar Data

Upon completion of data acquisition, NV5 Geospatial processing staff initiated a suite of automated and manual techniques to process the data into the requested deliverables. Processing tasks included GPS control computations, smoothed best estimate trajectory (SBET) calculations, kinematic corrections, calculation of laser point position, sensor, and data calibration for optimal relative and absolute accuracy, and lidar point classification (Table 9). Processing methodologies were tailored for the landscape. Brief descriptions of these tasks are shown in Table 10.

Table 9: ASPRS LAS classification standards applied to the Umatilla, Union, & Morrow dataset

Classification Number	Classification Name	Point Count	Classification Description
1	Default/Unclassified	292,192,214,937	Laser returns that are not included in the ground class, composed of vegetation and anthropogenic features
1-W	Edge Clip/Withheld	2,994,184,167	Laser returns at the outer edges of flightlines that are geometrically unreliable
2	Ground	51,657,371,776	Laser returns that are determined to be ground using automated and manual cleaning algorithms
7-W	Noise/Withheld	6,537,229,265	Laser returns that are often associated with artificial points below the ground surface
9	Water	39,017,559	Laser returns that are determined to be water using automated and manual cleaning algorithms
17	Bridge	2,031,676	Bridge decks
18-W	High Noise/Withheld	497,304,041	Laser returns that are often associated with birds or scattering from reflective surfaces
20	Ignored Ground	1,494,989	Ground points proximate to water's edge breaklines; ignored for correct model creation
21	Snow	1,628,188	Laser returns in the presence of snow.
22	Temporal Exclusion	633,290	Laser returns that are determined to be due to temporal differences in flightlines and are excluded from model creation.

Table 10: Lidar Processing Workflow

Lidar Processing Step	Software Used
Resolve kinematic corrections for aircraft position data using kinematic aircraft GPS, Applanix PPRTX data and static ground GPS data. Develop a smoothed best estimate of trajectory (SBET) file that blends post-processed aircraft position with sensor head position and attitude recorded throughout the survey.	POSPac MMS v.8.5
Calculate laser point position by associating SBET position to each laser point return time, scan angle, intensity, etc. Create raw laser point cloud data for the entire survey in *.las (ASPRS v. 1.4) format. Convert data to orthometric elevations by applying a geoid correction.	RiProcess v1.8.5
Using ground classified points per each flight line, test the relative accuracy. Perform automated line-to-line calibrations for system attitude parameters (pitch, roll, heading), mirror flex (scale) and GPS/IMU drift. Calculate calibrations on ground classified points from paired flight lines and apply results to all points in a flight line. Use every flight line for relative accuracy calibration.	BayesMap StripAlign v2.19
Import calibrated points into manageable blocks for editing.	TerraScan v.19.005
Classify resulting data to ground and other client designated ASPRS classifications (Table 9). Assess statistical absolute accuracy via direct comparisons of ground classified points to ground control survey data.	TerraScan v.19.005 TerraModeler v.19.003
Generate hydroflattened bare earth models as triangulated surfaces. Generate highest hit models as a surface expression of all classified points. Export all surface models as Cloud Optimized GeoTIFFs at a 0.5-meter pixel resolution.	TerraScan v. 19.005 Las Product Creator 3.6 (NV5 proprietary software) ArcMap v. 10.3.1
Export intensity images and swath separation images as Cloud Optimized GeoTIFFs at a 0.5-meter pixel resolution.	Las Product Creator 3.6 (NV5 proprietary software) ArcMap v. 10.3.1

Feature Extraction

Hydroflattening and Water's Edge Breaklines

Water bodies within the project area were flattened to a consistent water level. Bodies of water that were flattened include lakes and other closed water bodies with a surface area greater than 2 acres, all streams and rivers that are nominally wider than 30 meters, all non-tidal waters bordering the project, and select smaller bodies of water as feasible. The hydroflattening process eliminates artifacts in the digital terrain model caused by both increased variability in ranges or dropouts in laser returns due to the low reflectivity of water.

Hydroflattening of closed water bodies was performed through a combination of automated and manual detection and adjustment techniques designed to identify water boundaries and water levels. The water edges were then manually reviewed and edited as necessary.

Once polygons were developed the initial ground classified points falling within water polygons were reclassified as water points to omit them from the final ground model. Elevations were then obtained from the filtered lidar returns to create the final breaklines. Lakes were assigned a consistent elevation for an entire polygon while rivers were assigned consistent elevations on opposing banks and smoothed to ensure downstream flow through the entire river channel.

Water boundary breaklines were then incorporated into the hydroflattened DEM by enforcing triangle edges (adjacent to the breakline) to the elevation values of the breakline. This implementation corrected interpolation along the hard edge. Water surfaces were obtained from a TIN of the 3-D water edge breaklines resulting in the final hydroflattened model (Figure 5).

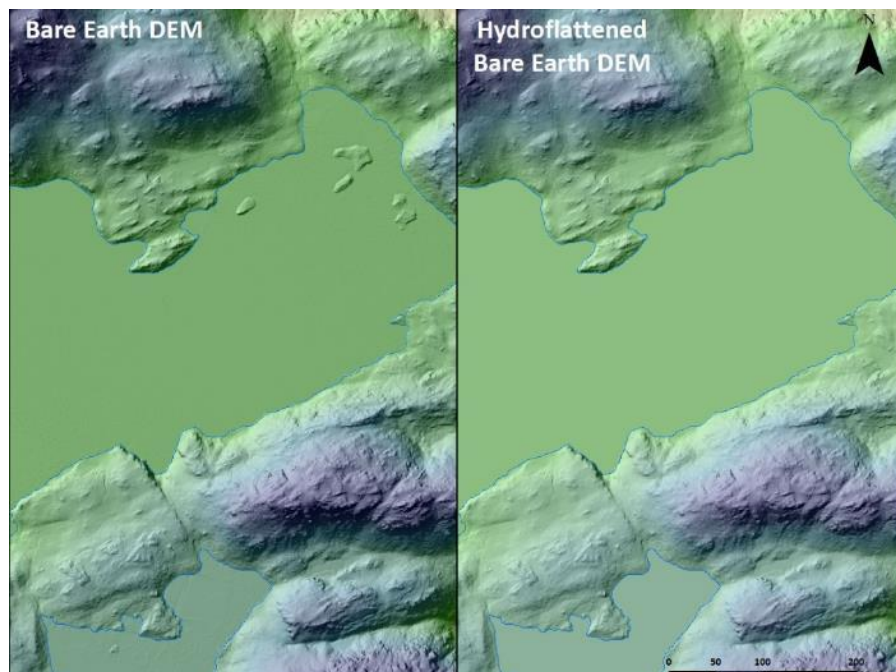
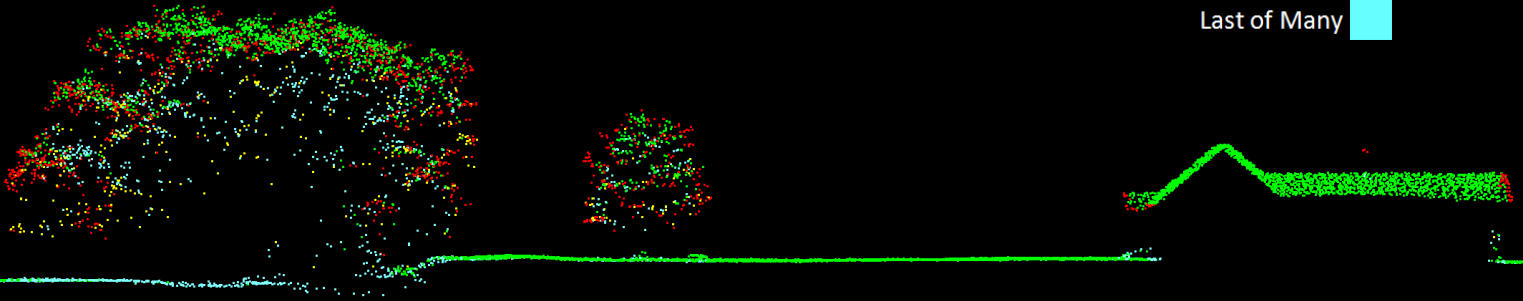


Figure 5: Example of hydroflattening in the Umatilla, Union, & Morrow Lidar dataset

This 2 meter lidar cross section shows the point returns from vegetation, bare ground, and a house in the 3DEP Umatilla, Union, and Morrow, Oregon AOI (colored by point laser echo).

Only Echo ■
 First of Many ■
 Intermediate ■
 Last of Many ■



Lidar Density

The acquisition parameters were designed to acquire an average first-return density of 8 points/m². First return density describes the density of pulses emitted from the laser that return at least one echo to the system. Multiple returns from a single pulse were not considered in first return density analysis. Some types of surfaces (e.g., breaks in terrain, water, and steep slopes) may have returned fewer pulses than originally emitted by the laser. First returns typically reflect off the highest feature on the landscape within the footprint of the pulse. In forested or urban areas, the highest feature could be a tree, building or power line, while in areas of unobstructed ground, the first return will be the only echo and represents the bare earth surface.

The density of ground-classified lidar returns was also analyzed for this project. Terrain character, land cover, and ground surface reflectivity all influenced the density of ground surface returns. In vegetated areas, fewer pulses may penetrate the canopy, resulting in lower ground density.

The average first-return density of lidar data for the Umatilla, Union, & Morrow project was 19.52 points/m², while the average ground classified density was 4.18 points/m² (Table 11). The statistical and spatial distributions of first return densities and classified ground return densities per 100 m x 100 m cell are portrayed in Figure 6 through Figure 9.

Table 11: Average lidar point densities

Classification	Point Density
First-Return	19.52 points/m ²
Ground Classified	4.18 points/m ²

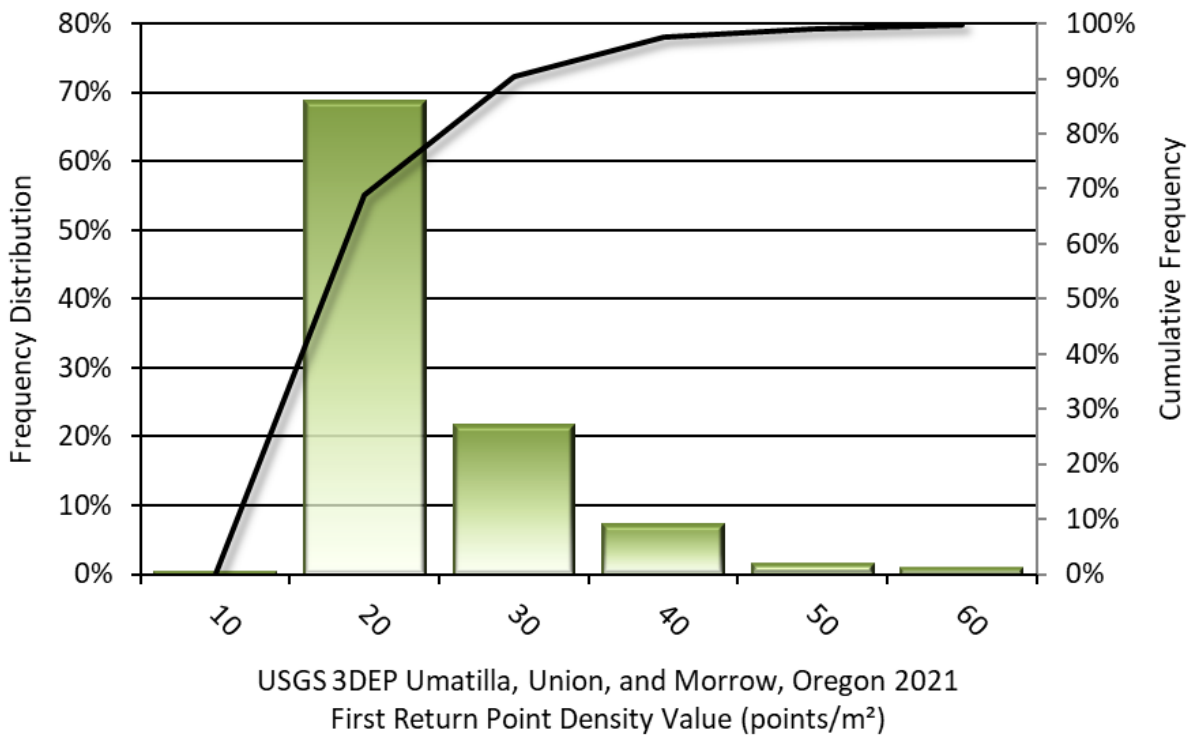


Figure 6: Frequency distribution of first return point density values per 100 x 100 m cell

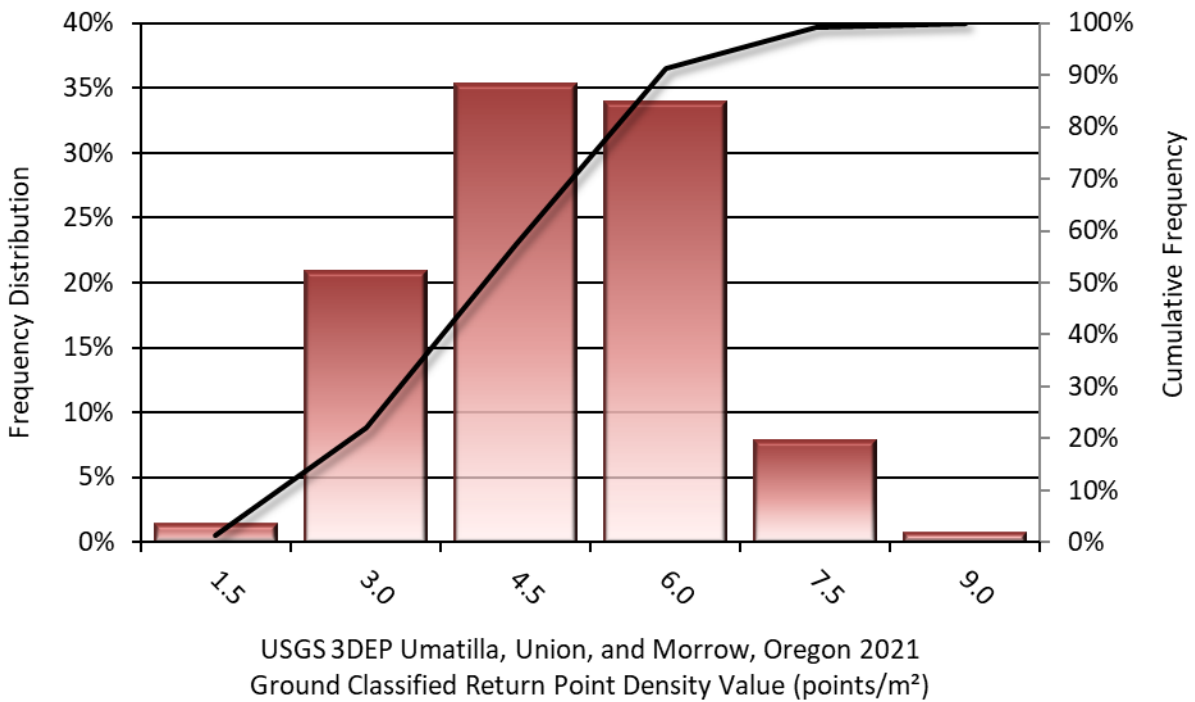


Figure 7: Frequency distribution of ground-classified return point density values per 100 x 100 m cell

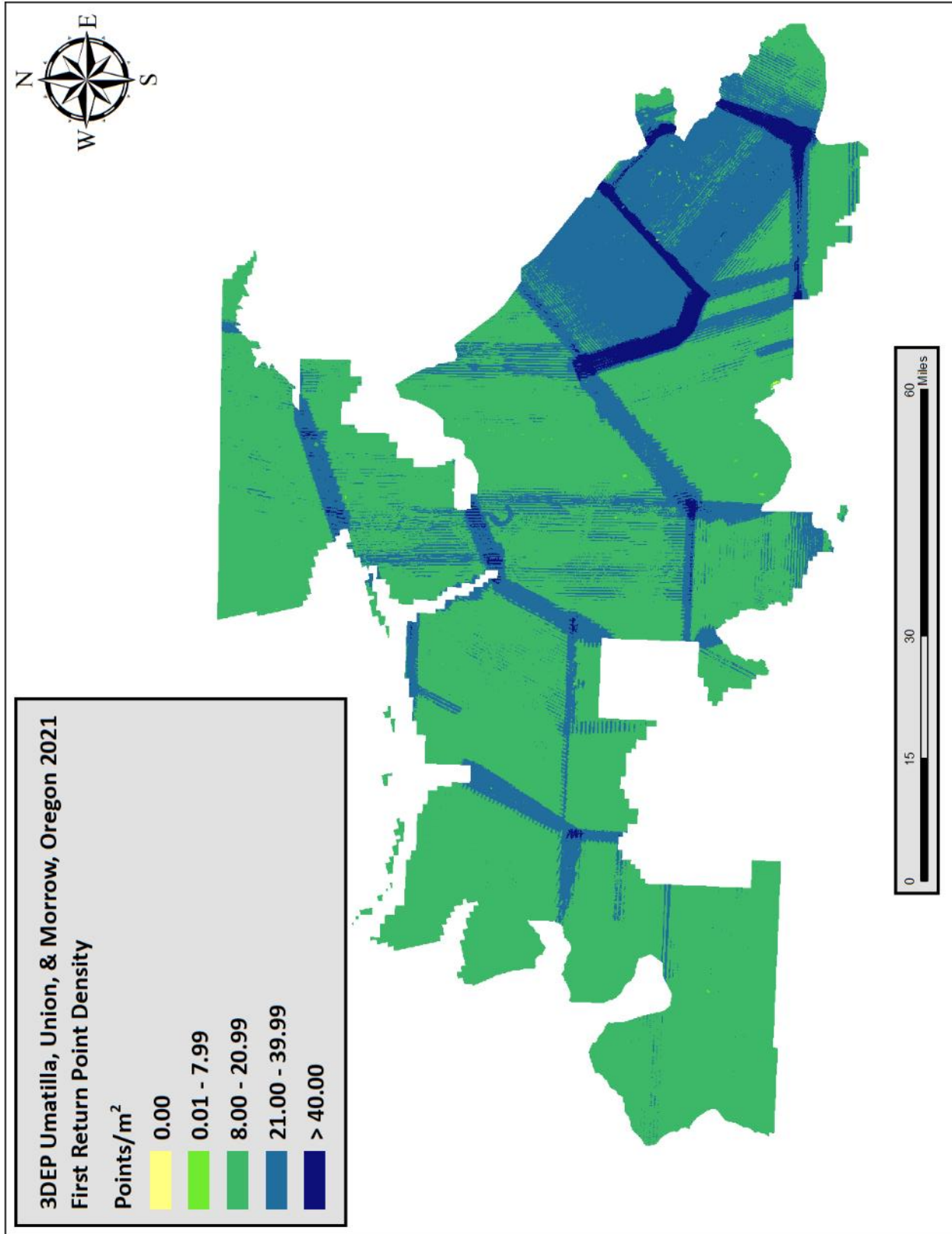


Figure 8: First return point density map for the Umatilla, Union, & Morrow site (100 m x 100 m cells)

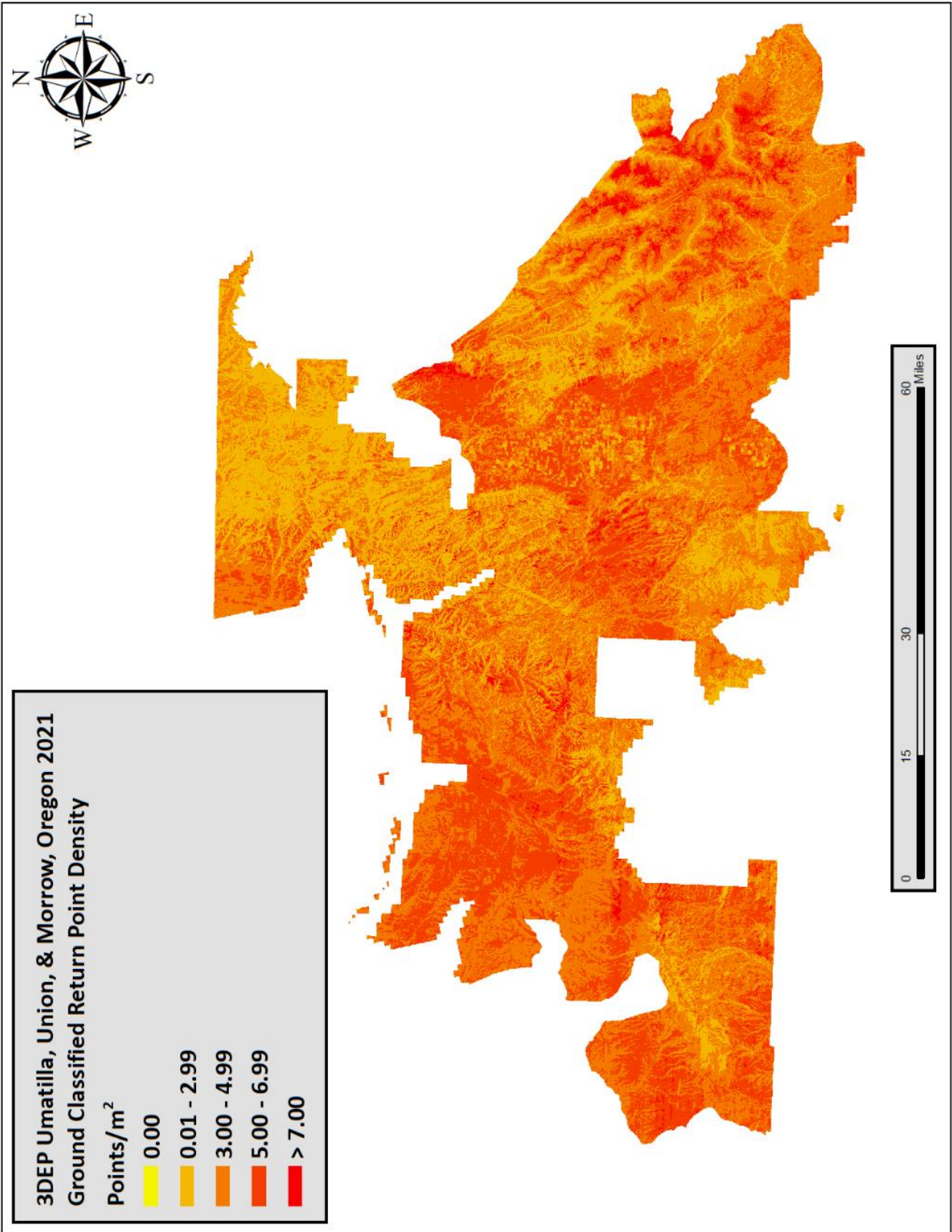


Figure 9: Ground point density map for the Umatilla, Union, & Morrow site (100 m x 100 m cells)

Lidar Accuracy Assessments

The accuracy of the lidar data collection can be described in terms of absolute accuracy (the consistency of the data with external data sources) and relative accuracy (the consistency of the dataset with itself). See Appendix A for further information on sources of error and operational measures used to improve relative accuracy.

Lidar Non-Vegetated Vertical Accuracy

Absolute accuracy was assessed using Non-Vegetated Vertical Accuracy (NVA) reporting designed to meet guidelines presented in the FGDC National Standard for Spatial Data Accuracy³. NVA compares known ground check point data that were withheld from the calibration and post-processing of the lidar point cloud to the triangulated surface generated by the classified lidar point cloud as well as the derived gridded bare earth DEM. NVA is a measure of the accuracy of lidar point data in open areas where the lidar system has a high probability of measuring the ground surface and is evaluated at the 95% confidence interval ($1.96 * RMSE$), as shown in Table 12.

The mean and standard deviation (sigma σ) of divergence of the ground surface model from quality assurance point coordinates are also considered during accuracy assessment. These statistics assume the error for x, y and z is normally distributed, and therefore the skew and kurtosis of distributions are also considered when evaluating error statistics. For the Umatilla, Union, & Morrow survey, 125 ground check points were withheld from the calibration and post processing of the lidar point cloud, with resulting non-vegetated vertical accuracy of 0.065 meters as compared to classified LAS, and 0.070 meters as compared to the bare earth DEM, with 95% confidence (Figure 10, Figure 11). The non-vegetated accuracy compared to the classified LAS and DEM both meet the QL1 criteria of 19.6 cm.

NV5 Geospatial also assessed absolute accuracy using 117 ground control points. Although these points were used in the calibration and post-processing of the lidar point cloud, they still provide a good indication of the overall accuracy of the lidar dataset, and therefore have been provided in Table 12 and Figure 12.

³ Federal Geographic Data Committee, ASPRS POSITIONAL ACCURACY STANDARDS FOR DIGITAL GEOSPATIAL DATA EDITION 1, Version 1.0, NOVEMBER 2014.

https://www.asprs.org/a/society/committees/standards/Positional_Accuracy_Standards.pdf.

Table 12: Absolute accuracy results

Non-Vegetated Vertical Accuracy			
	NVA, as compared to classified LAS	NVA, as compared to bare earth DEM	Ground Control Points
Sample	125 points	125 points	117 points
95% Confidence (1.96*RMSE)	0.065 m	0.070 m	0.067 m
Average	0.004 m	0.004 m	0.002 m
Median	0.003 m	-0.001 m	0.003 m
RMSE	0.033 m	0.036 m	0.034 m
Standard Deviation (1σ)	0.033 m	0.035 m	0.034 m

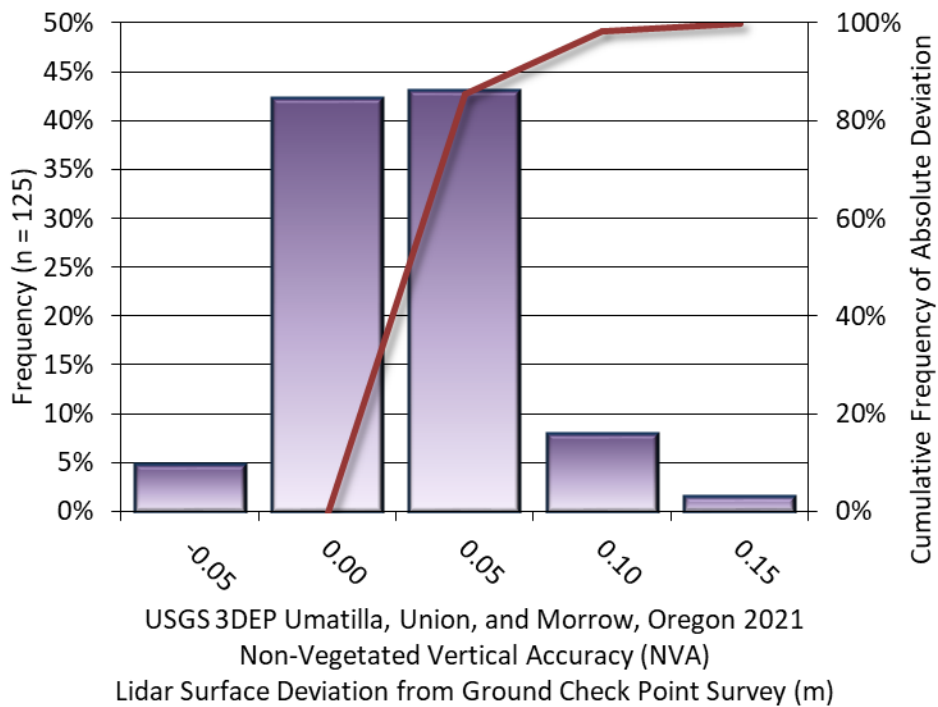


Figure 10: Frequency histogram for lidar classified LAS deviation from ground check point values (NVA)

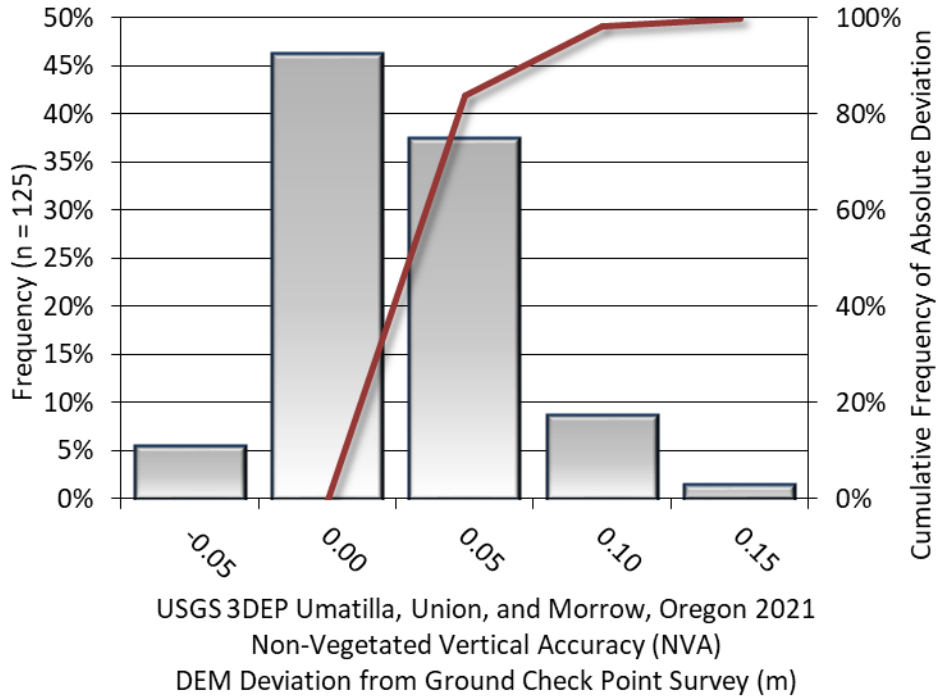


Figure 11: Frequency histogram for the lidar bare earth DEM surface deviation from ground check point values (NVA)

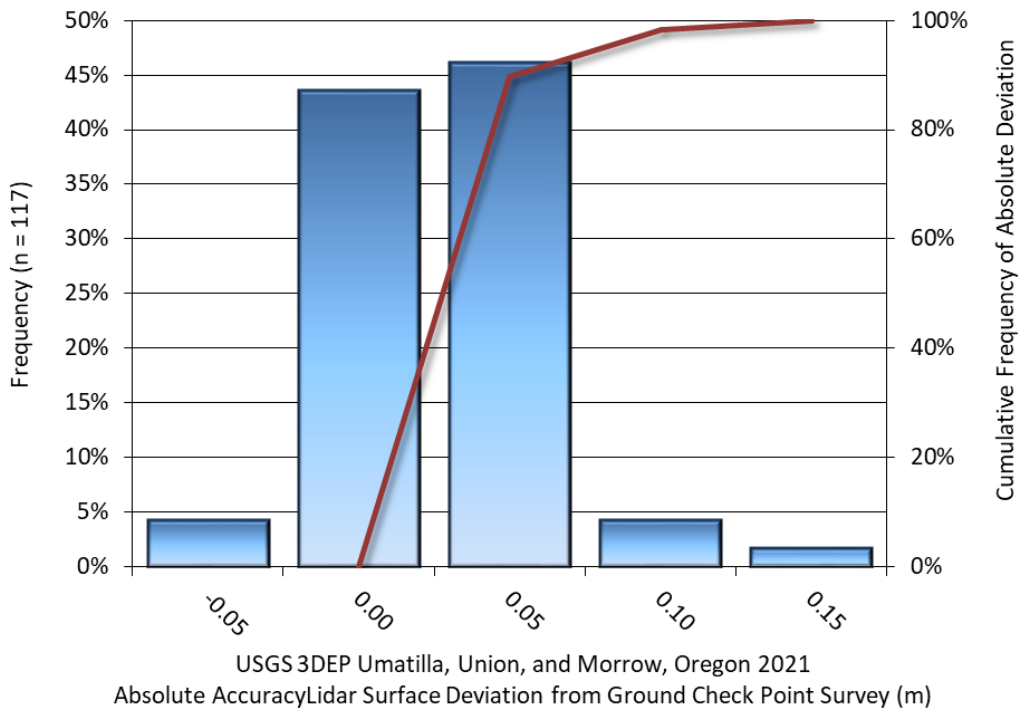


Figure 12: Frequency histogram for the lidar surface deviation from ground control point values

Lidar Vegetated Vertical Accuracies

NV5 geospatial also assessed vertical accuracy using Vegetated Vertical Accuracy (VVA) reporting. VVA compares known ground check point data collected over vegetated surfaces using land class descriptions to the triangulated ground surface generated by the ground classified lidar points. For the Umatilla, Union, & Morrow survey, 98 vegetated check points were collected, with resulting vegetated vertical accuracy of 0.176 meters as compared to the classified LAS, and 0.186 meters as compared to the bare earth DEM evaluated at the 95th percentile (Table 13, Figure 13, and Figure 14). These values are within QL1 criteria.

Table 13: Vegetated vertical accuracy results

Vegetated Vertical Accuracy		
	VVA, as compared to classified LAS	VVA, as compared to bare earth DEM
Sample	98 points	98 points
95 th Percentile	0.176 m	0.186 m
Average	0.049 m	0.051 m
Median	0.031 m	0.034 m
RMSE	0.085 m	0.086 m
Standard Deviation (1σ)	0.070 m	0.069 m

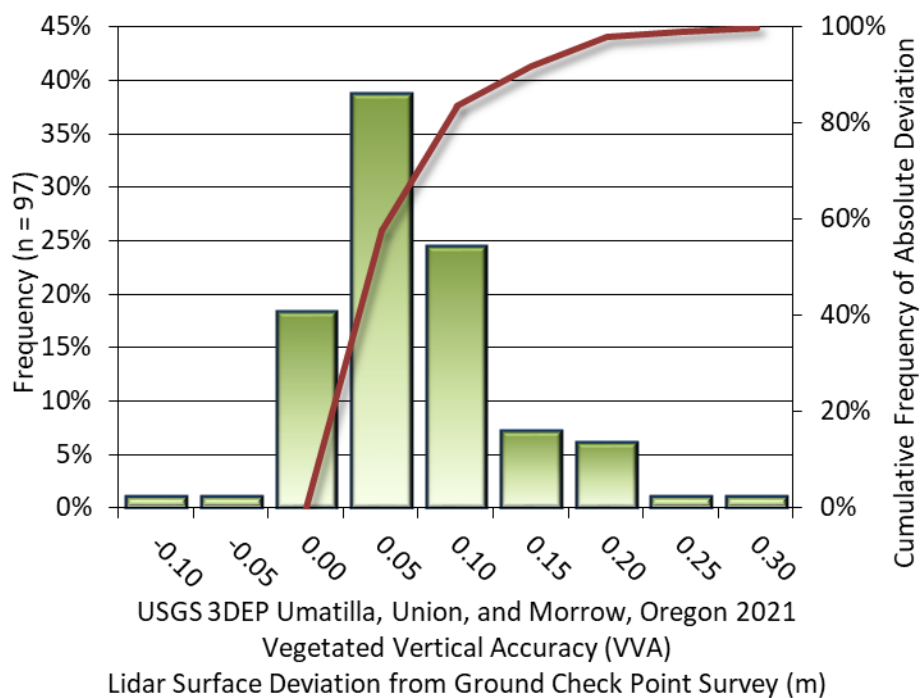


Figure 13: Frequency histogram for the lidar surface deviation from vegetated check point values (VVA)

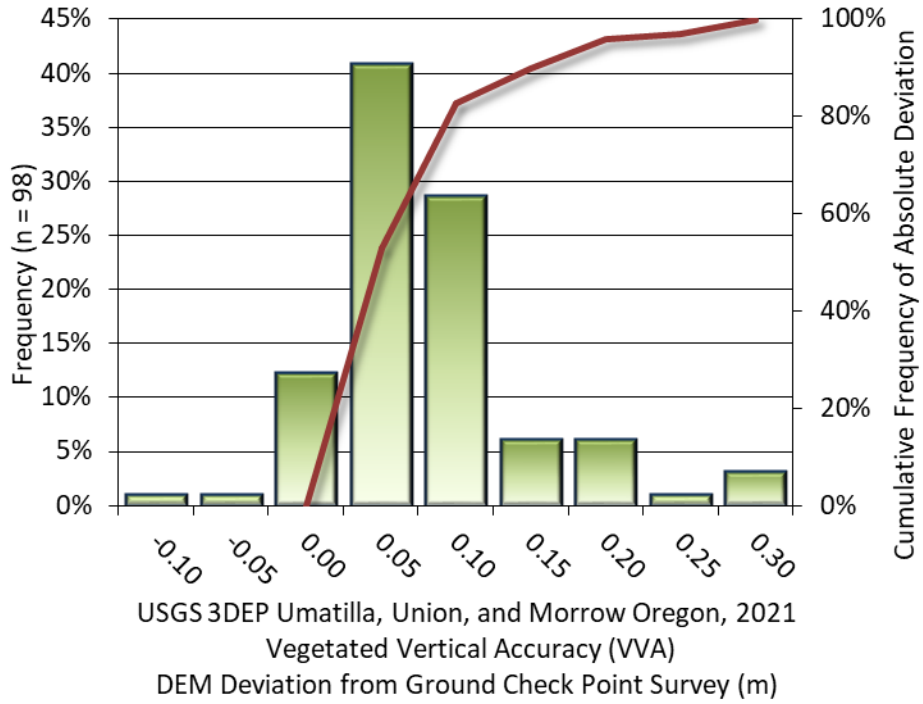


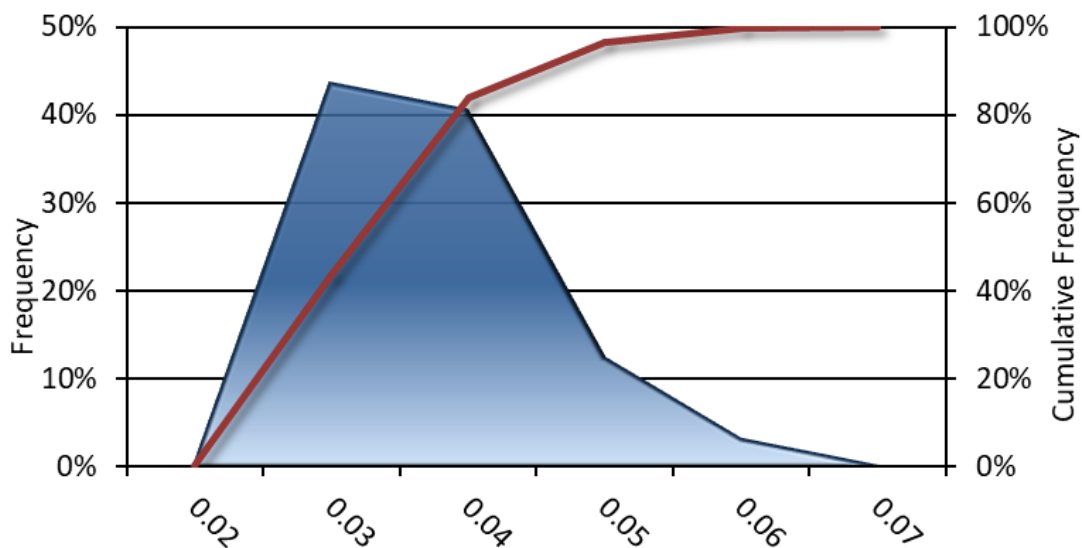
Figure 14: Frequency histogram for the lidar bare earth DEM deviation from vegetated check point values (VVA)

Lidar Relative Vertical Accuracy

Relative vertical accuracy refers to the internal consistency of the data set as a whole: the ability to place an object in the same location given multiple flight lines, GPS conditions, and aircraft attitudes. When the lidar system is well calibrated, the swath-to-swath vertical divergence is low (<0.10 meters). The relative vertical accuracy was computed by comparing the ground surface model of each individual flight line with its neighbors in overlapping regions. The average (mean) line to line relative vertical accuracy for the Umatilla, Union, & Morrow Lidar project was 0.030 meters (Table 14, Figure 15).

Table 14: Relative accuracy results

Relative Accuracy	
Sample	851 flight line surfaces
Average	0.030 m
Median	0.031 m
RMSE	0.033 m
Standard Deviation (1σ)	0.008 m
1.96σ	0.016 m



USGS 3DEP Umatilla, Union, and Morrow, Oregon 2021

Relative Vertical Accuracy (m)

Total Compared Points (n = 342,048,298,279)

Figure 15: Frequency plot for relative vertical accuracy between flight lines

Lidar Horizontal Accuracy

Lidar horizontal accuracy is a function of Global Navigation Satellite System (GNSS) derived positional error, flying altitude, and INS derived attitude error. The obtained $RMSE_r$ value is multiplied by a conversion factor of 1.7308 to yield the horizontal component of the National Standards for Spatial Data Accuracy (NSSDA) reporting standard where a theoretical point will fall within the obtained radius 95 percent of the time. Two different flying altitudes were used during this project.

Based on a flying altitude of 2,085 meters, an IMU error of 0.002 decimal degrees, and a GNSS positional error of 0.032 meters, this project was produced to meet 0.23 meters horizontal accuracy at the 95% confidence level.

Based on a flying altitude of 2,365 meters, an IMU error of 0.002 decimal degrees, and a GNSS positional error of 0.023 meters, this project was produced to meet 0.26 meters horizontal accuracy at the 95% confidence level.

Table 15: Horizontal Accuracy

Horizontal Accuracy		
Flying Altitude	2,085 m	2,365 m
$RMSE_r$	0.13 m	0.15 m
ACC_r	0.23 m	0.26 m

CERTIFICATIONS

NV5 Geospatial provided lidar services for the Umatilla, Union, & Morrow project as described in this report.

I, John English, have reviewed the attached report for completeness and hereby state that it is a complete and accurate report of this project.

John T. English

May 15, 2022

John English
Project Manager
NV5 Geospatial

I, Evon P. Silvia, PLS, being duly registered as a Professional Land Surveyor in and by the state of Oregon, hereby certify that the methodologies, static GNSS occupations used during airborne flights, and ground survey point collection were performed using commonly accepted Standard Practices. Field work conducted for this report was conducted between April 15 and September 3, 2021 for the airborne survey, and between April 23 and July 28, 2021 for the ground survey.

Accuracy statistics shown in the Accuracy Section of this Report have been reviewed by me and found to meet the "National Standard for Spatial Data Accuracy".

Evon P. Silvia

May 13, 2022

Evon P. Silvia, PLS
NV5 Geospatial
Corvallis, OR 97330

REGISTERED
PROFESSIONAL
LAND SURVEYOR

Evon P. Silvia

OREGON
JUNE 10, 2014
EVON P. SILVIA
81104LS

EXPIRES: 06/30/2022

GLOSSARY

1-sigma (σ) Absolute Deviation: Value for which the data are within one standard deviation (approximately 68th percentile) of a normally distributed data set.

1.96 * RMSE Absolute Deviation: Value for which the data are within two standard deviations (approximately 95th percentile) of a normally distributed data set, based on the FGDC standards for Non-vegetated Vertical Accuracy (NVA) reporting.

Accuracy: The statistical comparison between known (surveyed) points and laser points. Typically measured as the standard deviation (σ) and root mean square error (RMSE).

Absolute Accuracy: The vertical accuracy of lidar data is described as the mean and standard deviation (σ) of divergence of lidar point coordinates from ground survey point coordinates. To provide a sense of the model predictive power of the dataset, the root mean square error (RMSE) for vertical accuracy is also provided. These statistics assume the error distributions for x, y and z are normally distributed, and thus we also consider the skew and kurtosis of distributions when evaluating error statistics.

Relative Accuracy: Relative accuracy refers to the internal consistency of the data set; i.e., the ability to place a laser point in the same location over multiple flight lines, GPS conditions and aircraft attitudes. Affected by system attitude offsets, scale and GPS/IMU drift, internal consistency is measured as the divergence between points from different flight lines within an overlapping area. Divergence is most apparent when flight lines are opposing. When the lidar system is well calibrated, the line-to-line divergence is low (<10 cm).

Root Mean Square Error (RMSE): A statistic used to approximate the difference between real-world points and the lidar points. It is calculated by squaring all the values, then taking the average of the squares and taking the square root of the average.

Data Density: A common measure of lidar resolution, measured as points per square meter.

Digital Elevation Model (DEM): File or database made from surveyed points, containing elevation points over a contiguous area. Digital terrain models (DTM) and digital surface models (DSM) are types of DEMs. DTMs consist solely of the bare earth surface (ground points), while DSMs include information about all surfaces, including vegetation and man-made structures.

Intensity Values: The peak power ratio of the laser return to the emitted laser, calculated as a function of surface reflectivity.

Nadir: A single point or locus of points on the surface of the earth directly below a sensor as it progresses along its flight line.

Overlap: The area shared between flight lines, typically measured in percent. 100% overlap is essential to ensure complete coverage and reduce laser shadows.

Pulse Rate (PR): The rate at which laser pulses are emitted from the sensor; typically measured in thousands of pulses per second (kHz).

Pulse Returns: For every laser pulse emitted, the number of wave forms (i.e., echoes) reflected back to the sensor. Portions of the wave form that return first are the highest element in multi-tiered surfaces such as vegetation. Portions of the wave form that return last are the lowest element in multi-tiered surfaces.

Real-Time Kinematic (RTK) Survey: A type of surveying conducted with a GPS base station deployed over a known monument with a radio connection to a GPS rover. Both the base station and rover receive differential GPS data and the baseline correction is solved between the two. This type of ground survey is accurate to 1.5 cm or less.

Post-Processed Kinematic (PPK) Survey: GPS surveying is conducted with a GPS rover collecting concurrently with a GPS base station set up over a known monument. Differential corrections and precisions for the GNSS baselines are computed and applied after the fact during processing. This type of ground survey is accurate to 1.5 cm or less.

Scan Angle: The angle from nadir to the edge of the scan, measured in degrees. Laser point accuracy typically decreases as scan angles increase.

Native Lidar Density: The number of pulses emitted by the lidar system, commonly expressed as pulses per square meter.

APPENDIX A - ACCURACY CONTROLS

Relative Accuracy Calibration Methodology:

Manual System Calibration: Calibration procedures for each mission require solving geometric relationships that relate measured swath-to-swath deviations to misalignments of system attitude parameters. Corrected scale, pitch, roll and heading offsets were calculated and applied to resolve misalignments. The raw divergence between lines was computed after the manual calibration was completed and reported for each survey area.

Automated Attitude Calibration: All data were tested and calibrated using TerraMatch or StripAlign automated sampling routines. Ground points were classified for each individual flight line and used for line-to-line testing. System misalignment offsets (pitch, roll and heading) and scale were solved for each individual mission and applied to respective mission datasets. The data from each mission were then blended when imported together to form the entire area of interest.

Automated Z Calibration: Ground points per line were used to calculate the vertical divergence between lines caused by vertical GPS drift. Automated Z calibration was the final step employed for relative accuracy calibration.

Lidar accuracy error sources and solutions:

Type of Error	Source	Post Processing Solution
GPS (Static/Kinematic)	Long Base Lines	None
	Poor Satellite Constellation	None
	Poor Antenna Visibility	Reduce Visibility Mask
Relative Accuracy	Poor System Calibration	Recalibrate IMU and sensor offsets/settings
	Inaccurate System	None
Laser Noise	Poor Laser Timing	None
	Poor Laser Reception	None
	Poor Laser Power	None
	Irregular Laser Shape	None

Operational measures taken to improve relative accuracy:

Low Flight Altitude: Terrain following was employed to maintain a constant above ground level (AGL). Laser horizontal errors are a function of flight altitude above ground (about 1/3000th AGL flight altitude).

Focus Laser Power at narrow beam footprint: A laser return must be received by the system above a power threshold to accurately record a measurement. The strength of the laser return (i.e., intensity) is a function of laser emission power, laser footprint, flight altitude and the reflectivity of the target. While surface reflectivity cannot be controlled, laser power can be increased and low flight altitudes can be maintained.

Reduced Scan Angle: Edge-of-scan data can become inaccurate. The scan angle was reduced to a maximum of $\pm 29.25^\circ$ from nadir, creating a narrow swath width and greatly reducing laser shadows from trees and buildings.

Quality GPS: Flights took place during optimal GPS conditions (e.g., 6 or more satellites and PDOP [Position Dilution of Precision] less than 3.0). Before each flight, the PDOP was determined for the survey day. During all flight times, a dual frequency DGPS base station recording at 1 second epochs was utilized and a maximum baseline length between the aircraft and the control points was less than 13 nm at all times.

Ground Survey: Ground survey point accuracy (<1.5 cm RMSE) occurs during optimal PDOP ranges and targets a minimal baseline distance of 4 miles between GPS rover and base. Robust statistics are, in part, a function of sample size (n) and distribution. Ground survey points are distributed to the extent possible throughout multiple flight lines and across the survey area.

50% Side-Lap (100% Overlap): Overlapping areas are optimized for relative accuracy testing. Laser shadowing is minimized to help increase target acquisition from multiple scan angles. Ideally, with a 50% side-lap, the nadir portion of one flight line coincides with the swath edge portion of overlapping flight lines. A minimum of 50% side-lap with terrain-followed acquisition prevents data gaps.

Opposing Flight Lines: All overlapping flight lines have opposing directions. Pitch, roll and heading errors are amplified by a factor of two relative to the adjacent flight line(s), making misalignments easier to detect and resolve.